Monthly Notices
of the
ROYAL ASTRONOMICAL SOCIETY

MNRAS **451,** 1117–1129 (2015) doi:10.1093/mnras/stv1039

Formation of a rotating jet during the filament eruption on 2013 April 10–11

B. Filippov,[1]★ A. K. Srivastava,[2] B. N. Dwivedi,[2] S. Masson,[3] G. Aulanier,[3] N. C. Joshi[4] and W. Uddin[5]

[1]*Pushkov Institute of Terrestrial Magnetism, Ionosphere and Radio Wave Propagation of the Russian Academy of Sciences (IZMIRAN), Troitsk, Moscow 142190, Russia*
[2]*Department of Physics, Indian Institute of Technology, Banaras Hindu University, Varanasi 221005, India*
[3]*LESIA, Observatoire de Paris, CNRS, UPMC, Univ. Paris Diderot, 5 place Jules Janssen, F-92190 Meudon, France*
[4]*School of Space Research, Kyung Hee University, Yongin, Gyeonggi-Do 446-701, Korea*
[5]*Aryabhatta Research Institute of Observational Sciences (ARIES), Manora Peak, Nainital 263009, India*

Accepted 2015 May 6. Received 2015 May 4; in original form 2015 April 3

ABSTRACT

We analyse multiwavelength and multiviewpoint observations of a helically twisted plasma jet formed during a confined filament eruption on 2013 April 10–11. Given a rather large-scale event with its high spatial and temporal resolution observations, it allows us to clearly understand some new physical details about the formation and triggering mechanism of twisting jet. We identify a pre-existing flux rope associated with a sinistral filament, which was observed several days before the event. The confined eruption of the filament within a null-point topology, also known as an Eiffel tower (or inverted-Y) magnetic field configuration results in the formation of a twisted jet after the magnetic reconnection near a null point. The sign of helicity in the jet is found to be the same as that of the sign of helicity in the filament. Untwisting motion of the reconnected magnetic field lines gives rise to the accelerating plasma along the jet axis. The event clearly shows the twist injection from the pre-eruptive magnetic field to the jet.

Key words: Sun: activity – Sun: filaments, prominences – Sun: magnetic fields.

1 INTRODUCTION

Among the different types of plasma motions observed during solar eruptive events in the corona and chromosphere, there are apparently linear collimated plasma flows, which are presumably guided by magnetic fields, usually referred to as jets. A wide variety of jet-like structures are observed in the solar atmosphere. They can be formed both from relatively cool plasma such as spicules, spikes, macro-spicules and surges and from hot plasma as seen in X-rays, white-light and Extreme Ultraviolet (EUV). Numerous small-scale jets are observed by *Hinode*/X-ray telescope.

While the general shape of jets is a nearly straight or slightly curved linear structure, high resolution and spectral observations reveal complicated motions within many jets. Rotation about the jet axis (spinning) and helical features were noticed long ago in spicules (Cook et al. 1984; Pike & Mason 1998; Sterling, Harra & Moore 2010), surges (Xu, Yin & Ding 1984; Kurokawa et al. 1987; Canfield et al. 1996) and jets (Shimojo et al. 1996; Patsourakos et al. 2008; Liu et al. 2009, 2011; Shen et al. 2011; Chen, Zhang & Ma 2012; Schmieder et al. 2013). Such plasma flow behaviour can be expected in pre-existing twisted coronal magnetic flux tubes or due to changes in the magnetic field during jet progress. In the interpretation of low spatio-temporal resolution observations, it is not easy to make right choice between these two possibilities.

Nevertheless, the major characteristic of jets is collimated field-aligned plasma motion. Plasma can be accelerated by the gas pressure gradient force, which is enhanced by sudden heating in the upper chromosphere (Steiolfson, Schmahl & Wu 1979; Suematsu et al. 1982), by the magnetic pressure force in a relaxing magnetic twist (Shibata & Uchida 1986), or by the magnetic tension force in the reconnection process (Shibata et al. 1992; Shibata 1998). Different models of jet formation based on reconnection have been proposed in two-dimensional (2D) and three-dimensional (3D) geometry (Yokoyama & Shibata 1996; Isobe, Tripathi & Archontis 2007; Pariat, Antiochos & DeVore 2010). Since the field line reconnection is most favorable near magnetic null points, magnetic configurations called as anemone-like, Eiffel tower, inverted-Y-shaped ones containing null points are often considered as source regions for jets. Reconnection is believed to be driven by emergence of a new magnetic flux from below the photosphere. The emergence time-scale is very slow compared with the time-scale of a jet

★E-mail: bfilip@izmiran.ru

phenomenon. Therefore, reconnection should be forbidden during the initial phase of the flux emergence by low plasma resistivity (Shibata, Nozawa & Matsumoto 1992) or high symmetry (Pariat, Antiochos & DeVore 2009). In this phase, a large amount of free magnetic energy is built up in the corona due to the formation of current sheets. The reconnection is switched on by anomalous resistivity or breaking the symmetry, which leads to an explosive release of the free energy.

Some new jet observations are inconsistent in several features with a 'standard' scenario of jet formation when a bipolar magnetic structure emerges into a pre-existing open magnetic field and reconnects to form hot and fast outflows that are emitted from the interface between the fields into contact (Heyvaerts, Priest & Rust 1977). They were called 'blowout jets' (Moore et al. 2010; Sterling et al. 2010; Liu et al. 2011; Shen et al. 2012). Blowout jets are broad, curtain-like structures in contrast to 'standard' jets, which are more elongated and contracting. In addition to the X-ray emitting plasma, cooler plasma at chromospheric or transition region temperatures erupts along these jets. The observed structure and timing of these cooler ejecta suggest that this plasma is erupted from low in the jet's base arch, in an ejective eruption of the magnetic field in the core of the arch as in a filament eruption and in a coronal mass ejection (CME). It is believed that there is a twisted or a sheared arch in the source region of a blowout jet, which often carries a small filament or flux rope within it. When this structure becomes unstable and erupts, it blows out the envelope field producing an untwisting ejection of cool and hot material.

3D magnetohydrodynamic simulations of the formation of jets (Archontis & Hood 2013) show that external reconnection between emerging and ambient magnetic field is important to turn on the standard jets, while the eruption of a sheared field within the emerging region and internal reconnection are key processes to form a twisted flux rope which is at the origin of the blowout jet. Field lines are twisted along the jet as a result of reconnection between the eruptive twisted field and the pre-existing field, which consists of non-twisted oblique field lines. Therefore, simulations show an untwisting plasma motion during the emission of the blowout jet. In another numerical experiment (Moreno-Insertis & Galsgaard 2013), the launching of a hot and fast coronal jet is followed by several violent eruptions. After the standard jet phase with the reconnection process that takes place at the interface between the colliding flux systems, a number of violent eruptions of the magnetic field structure take place in different volumes of the emerged plasma dome. Eruptions are possibly caused by a kink or torus instability. During a flux rope expanding in height, its twist turns into writhe. Pariat et al. (2015) studied the impact of the magnetic field inclination and photospheric field distribution on the generation and properties of straight and helical solar jets. They found that the 3D magnetic null-point configuration is a very robust structure for the energy storage and impulsive release characteristic of helical jets. Reconnection occurring during the straight-jet phase influences the triggering of the helical jet.

In this paper, we analyse new multiwavelength and multiviewpoint observations of a helically twisted plasma jet formed during a confined filament eruption on 2013 April 10–11. A rather large scale of the event and high spatial and temporal resolution of the *Solar Dynamic Observatory*/Atmospheric Imaging Assembly (*SDO*/AIA; Lemen et al. 2012) allow us to observe clearly some comprehensive and new details of the jet formation. In Section 2, we discuss general topology of the jet forming region. Dynamics and fine structure of the observed jet is described and analysed in Section 3. Last section presents some discussions.

2 GENERAL TOPOLOGY OF THE JET SOURCE REGION

For this study, we have used multiwavelength data from the AIA and the Heliospheric and Magnetic Imager (HMI; Schou et al. 2012) onboard the *SDO*, the Sun Earth Connection Coronal and Heliospheric Investigation (SECCHI) Extreme Ultraviolet Imager (EUVI; Wuelser et al. 2004; Howard et al. 2008) on board the *Solar Terrestrial Relations Observatory – Ahead* (*STEREO-A*), the Large Angle and Spectrometer Coronagraph (LASCO; Brueckner et al. 1995) on board the *Solar and Heliospheric Observatory* (*SOHO*), and ground-based full disc Hα observations of the Kanzelhoehe Solar Observatory. Observations from both the *STEREO-A*/SECCHI and *SDO*/AIA provide a good opportunity to study a jet phenomenon and associated dynamics on the disc as well as on the limb. The separation angle of the *STEREO-A* with the Earth was 134° on 2013 April 10–11, accordingly a feature observed by the *SDO* on the limb was located about 45° from the central meridian for the *STEREO-A*.

Fig. 1 shows the images of the Sun in the *STEREO*/EUVI 195 Å (top panel) and *SDO*/AIA 304 Å (bottom panel) channels with boxes showing the region of jet-like ejection around 23:00 UT on 2013 April 10. Left-hand panels show the full disc images of the Sun, while the right-hand panels show the zoomed images of the area corresponding to the boxes in the left-hand panels (the zoomed *STEREO*/EUVI image is in negative colour). The jet was associated with small National Oceanic and Atmospheric Administration (NOAA) active region 1715 located to the north-west from more developed NOAA active region 1713. NOAA 1715 active region lies near the coronal hole identified as a dark area in the *STEREO*/EUVI 195 Å full disc image (top-left panel of Fig. 1). The shape of coronal loops appears as an Eiffel tower or inverted-Y magnetic configuration of the jet source region. We can distinguish a fan surface and a spine in both *STEREO* and *SDO* images, which are shown by thin dashed white lines in Fig. 1. A null point should exist at the intersection of the fan surface and the spine. The coronal loops that outline the magnetic configuration change insignificantly for many hours before and after the jet event, which indicates the stability of the configuration. The studied jet event is only an episode in the life of this region, which does not destroy its topology.

SDO/HMI photospheric magnetograms on 2013 April 7, 8 and 9 (Fig. 2, upper panel) show a patch of positive polarity surrounded by a large area of negative polarity in this active region. The coronal-hole base is also located in a negative polarity region. The polarity inversion line (PIL) associated with this region (the dashed line in Fig. 3) is nearly circular and the connectivity between the positive and the negative fluxes displays an anemone-like shape. The potential-field source surface (PFSS) magnetic field extrapolation (Altschuler & Newkirk 1969; Schatten, Wilcox & Ness 1969; Schrijver & DeRosa 2003) confirms the presence of a null-point magnetic topology above NOAA 1715 active region (Fig. 2, bottom panel). High black lines connect NOAA 1715 active region with other regions and do not belong to the fan–spine configuration. They are so high, therefore, they can be considered as open field lines. The span of the fan surface in the SDO images is about 0.15 solar radii, while the span of the closed loop system in Fig. 2 is about 0.5 solar radii. In the bottom-left panel of Fig. 1, it is seen that the spine is close to the northern border of the structure. Therefore, the southern half of the calculated loop system is only two times wider than the southern half of the observed fan surface. We consider this as rather good agreement taking into account rather low spatial resolution of the PFSS magnetic field extrapolation and position of the

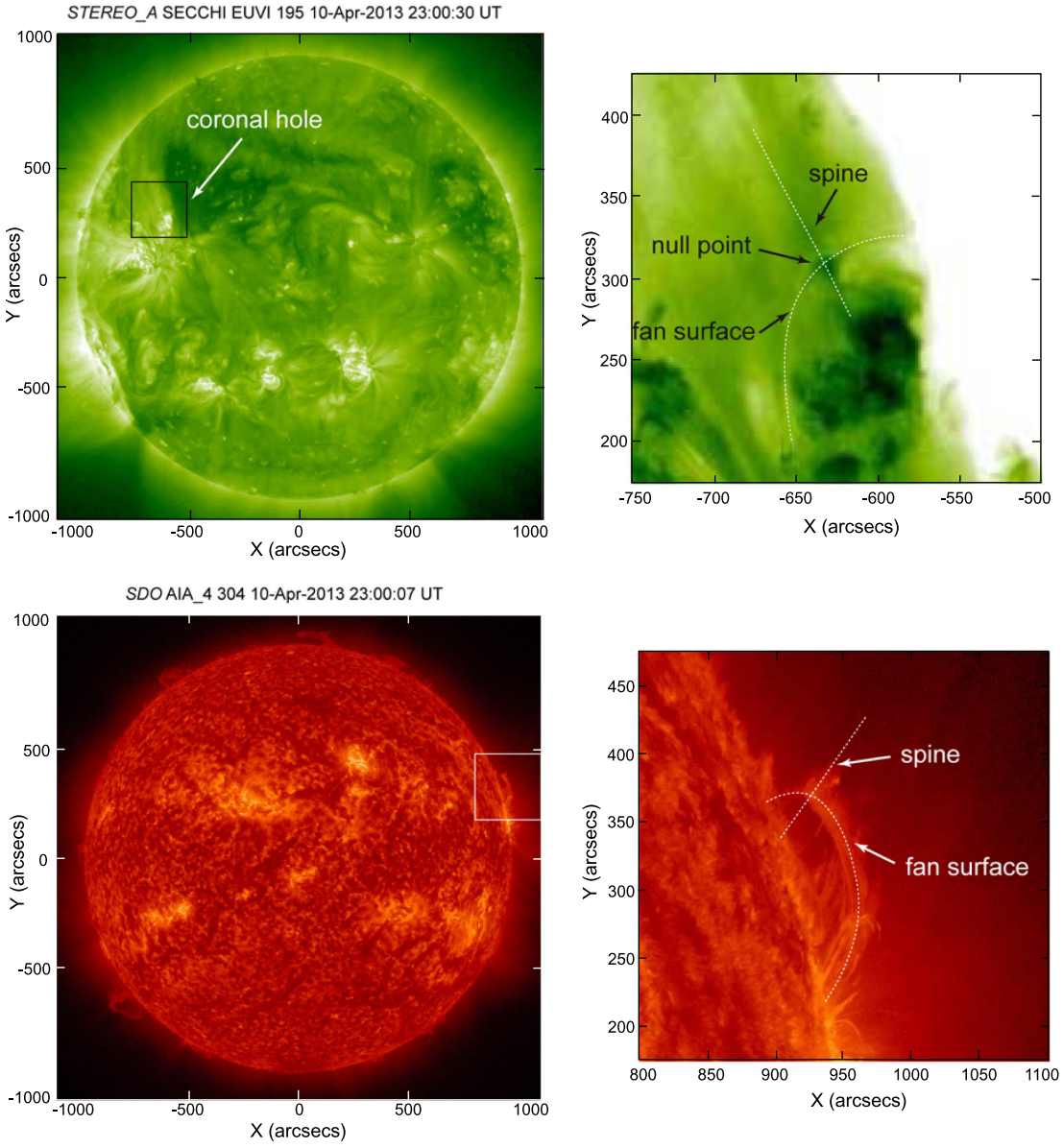

Figure 1. Full disc *STEREO*/SECCHI/EUVI 195 Å (top left), *SDO*/AIA 304 Å (bottom left) images and zoomed areas (right-hand panels) within boxes shown in left-hand panels.

studied active region close to the limb (magnetic field in the region cannot be measured on the day of jet observations).

The closed flux is confined within a dome, the boundary surface of which is the fan surface. Magenta lines (grey in black and white images) represent the coronal-hole open field lines. According to the directivity of the jet material, the outer spine is more likely open and belongs to the coronal hole, but it could also be alternatively closed among the large scale closed black field lines south of the null point (Wang & Liu 2012). Such null-point topology agrees very well with the *STEREO* and *SDO* observations highlighting an Eiffel tower configuration. Some details of pre-eruptive configuration of the source region are not very clear because of the position of the region being close to the limb in both *SDO* and ground-based observations. They are evidently clear only during the dynamical evolution of the event.

A faint filament within NOAA 1715 active region can be recognized in the Hα filtergram taken at 09:52 UT on 2013 April 08 at the Kanzelhoehe Solar Observatory (Fig. 3). It is stretched along the border of the patch of positive polarity within a large area of negative polarity, which constitutes the base of a coronal hole. There are stronger concentrations of negative polarity to the south-west from the positive patch. However, it is not easy to identify the polarity of each end of the filament where it is connected. It is likely that the northern end of the filament is connected to positive polarity, while the southern end is connected to negative polarity. This conclusion is proven during the eruption of the filament when the southern end remains connected to the surface, while the northern part of the filament forms a jet opening into the negative coronal hole. However, this filament end connectivity means the sinistral chirality of the filament, which is not typical for the Northern hemisphere. The hemispheric chirality rule is not strictly absolute (Pevtsov, Balasubramaniam & Roger 2003) and the conditions of its violation must be carefully analysed. The case of our filament seems to be exception from the general hemispheric chirality rule.

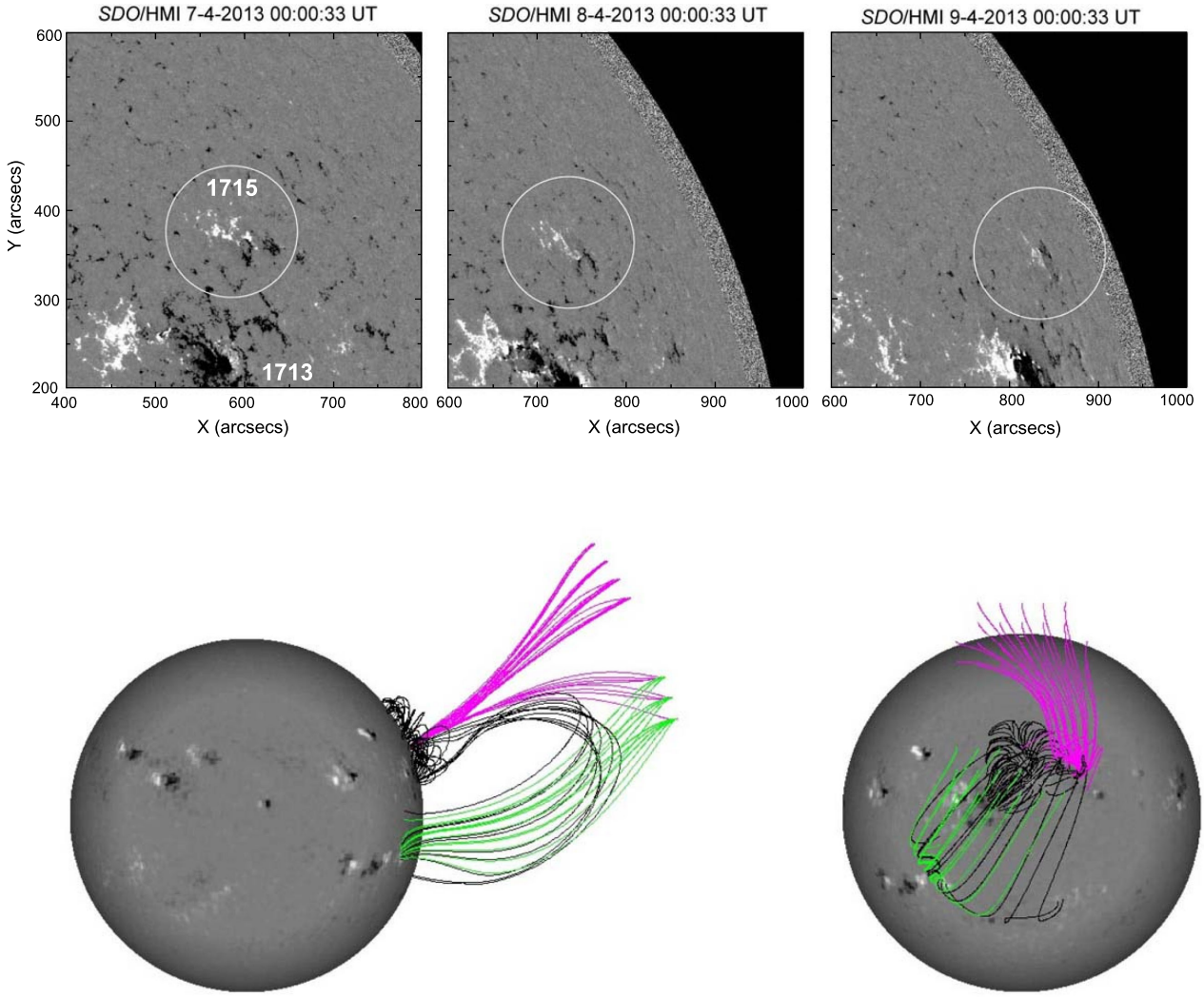

Figure 2. Upper panel: *SDO*/HMI fragments of line-of-sight magnetograms on 2013 April 7, 8 and 9. White circles show the location of NOAA 1715 active region. Bottom panel: PFSS magnetic field extrapolation showing a side view (left image) and a top view (right image) of the coronal magnetic field structure over NOAA 1715 active region. Magenta lines (grey in black and white images) represent open coronal-hole field lines. Green lines (light grey in black and white images) represent open field lines emanating from the Southern hemisphere.

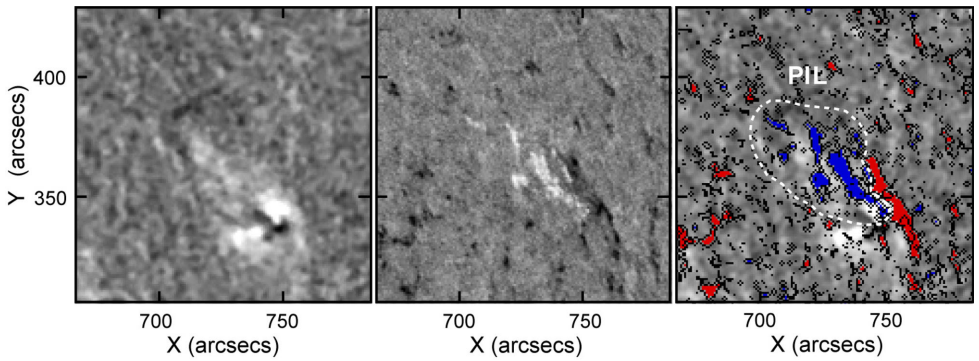

Figure 3. A fragment of the Hα filtergram taken at 09:52 UT on April 08 at the Kanzelhoehe Solar Observatory (left-hand panel), *SDO*/HMI magnetogram of the same region (central panel), Hα filtergram with overlaid +50 gauss (G) magnetic field contours from the *SDO*/HMI magnetogram (right-hand panel). Red areas (light grey in the black and white image) represent negative polarity, while blue areas (dark grey in the black and white image) represent positive polarity. The white dashed line shows PIL.

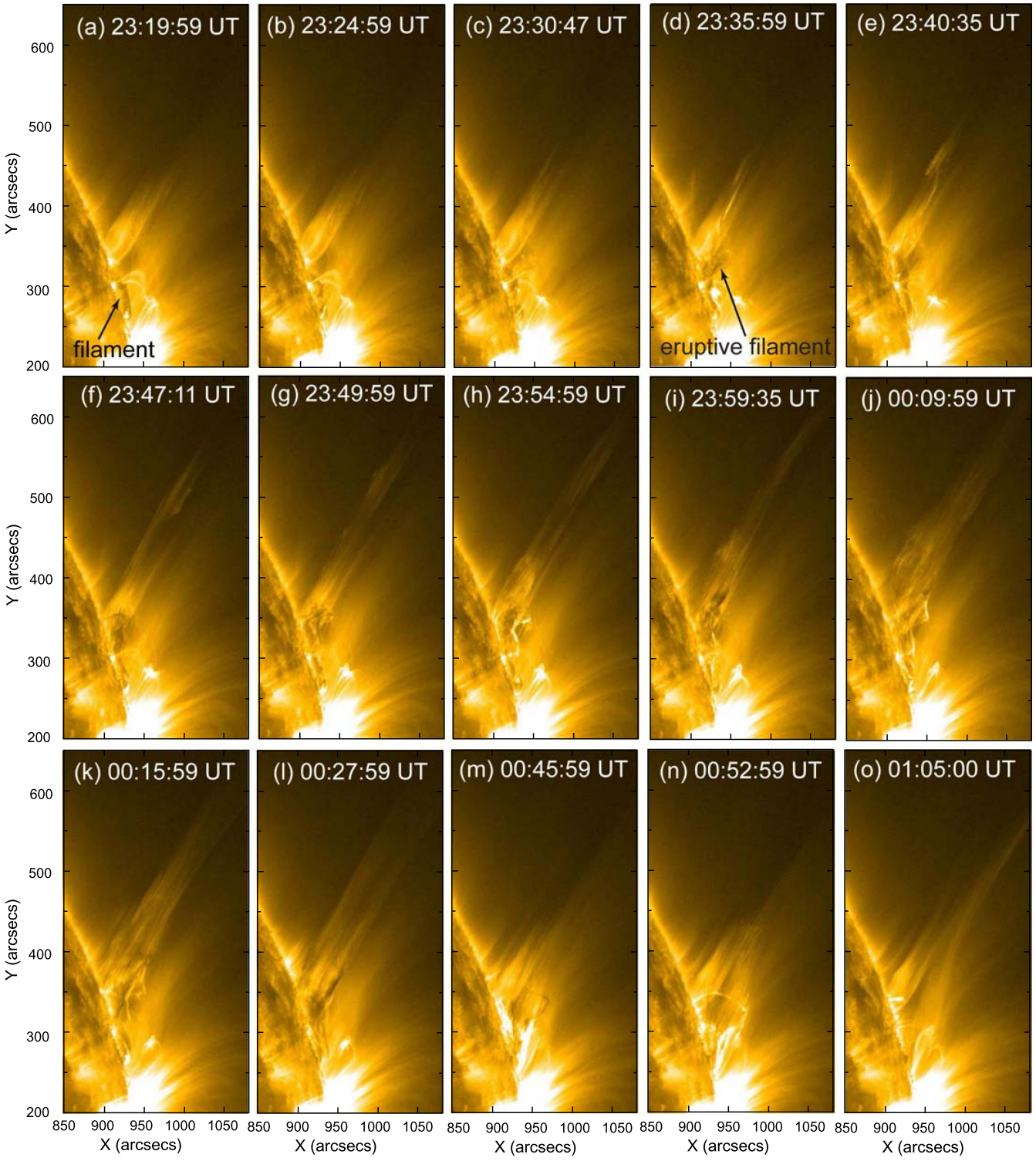

Figure 4. Sequence of selected *SDO*/AIA 171 Å images showing a filament eruption and formation of a set of three successive helically twisted jets.

The filament is clearly visible above the limb in *SDO*/AIA 171 Å images on 2013 April 10 as a dark absorbing feature with the top at a height of 13 Mm (Fig. 4 a). However, it is not visible in *SDO*/AIA 304 Å images before the first filament activation at 23:20 UT when the first brightening appears within the filament body.

Analysis of *SDO* and *STEREO-A* EUV images and photospheric magnetic field distribution shows that we have an Eiffel tower or inverse Y magnetic configuration in the corona (e.g. Shibata 1998) with a null point. The fan surface is outlined by stable loops in *SDO*/AIA 304 Å images (Figs 1 and 5) with anchored southern ends and suspended northern ends just near the probable null-point position. The direction of the spine slightly inclined to the north from the vertical becomes obvious after the jet formation, although it can be vaguely recognized from the direction of long straight loops

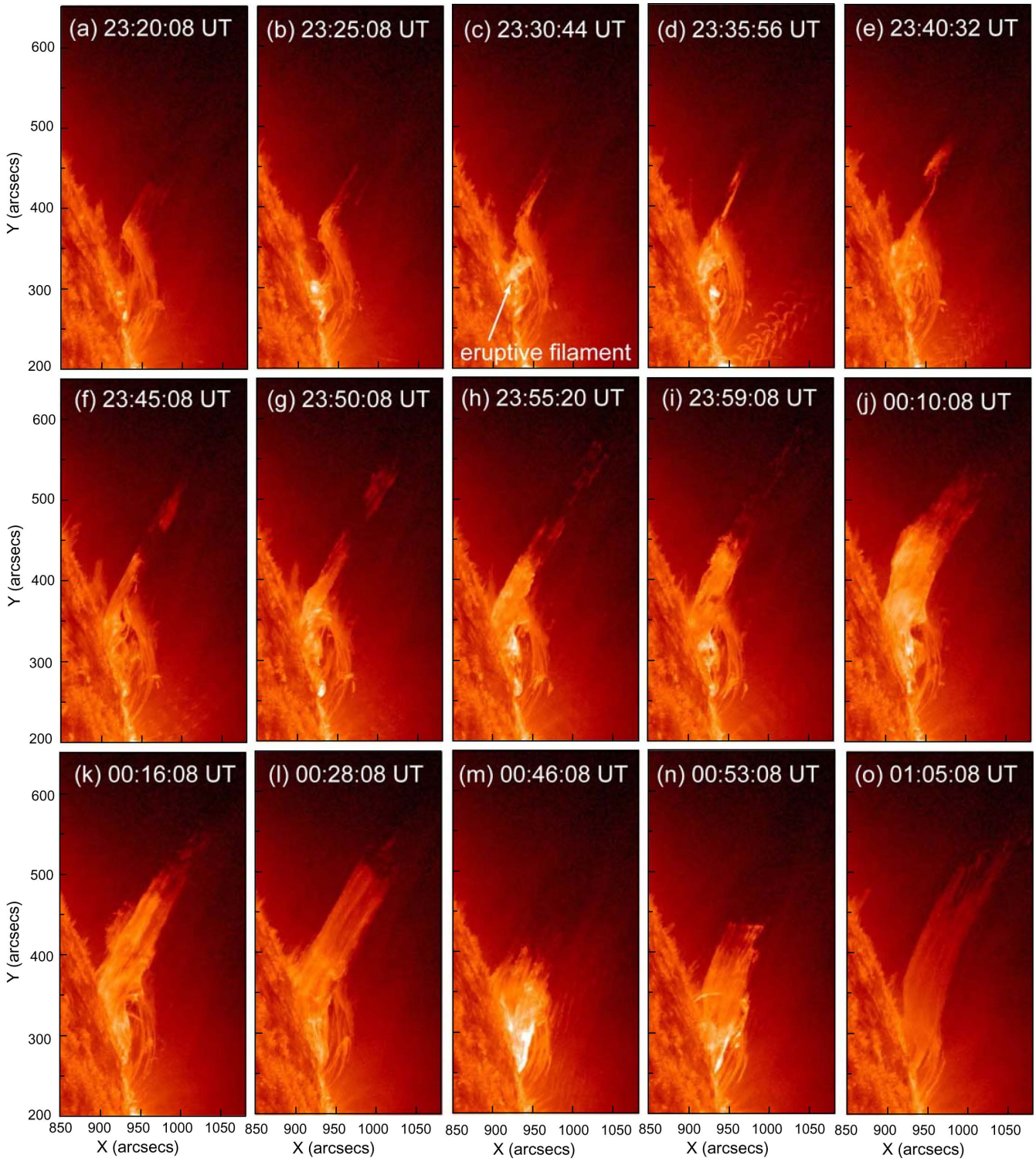

Figure 5. Sequence of selected *SDO*/AIA 304 Å images showing a filament eruption and formation of a set of three successive helically twisted jets.

visible in *SDO*/AIA 171 Å images on the background (Fig. 4). From the 304 Å image at 23:35:56 UT, we can estimate a height of the null point above the limb and the size of the dome along the limb as 40 and 100 Mm, respectively.

PFSS magnetic field extrapolation (Fig. 2) supports the schematic magnetic configuration shown in Fig. 6. Open field lines belonging to the coronal hole are shown with the magenta colour (grey in black and white images) in both figures, while closed field lines below the fan surface are black. One of the helical field lines composing a flux rope, which contains the filament, is shown with the blue colour before it becomes open after the jet formation and obtains the magenta colour.

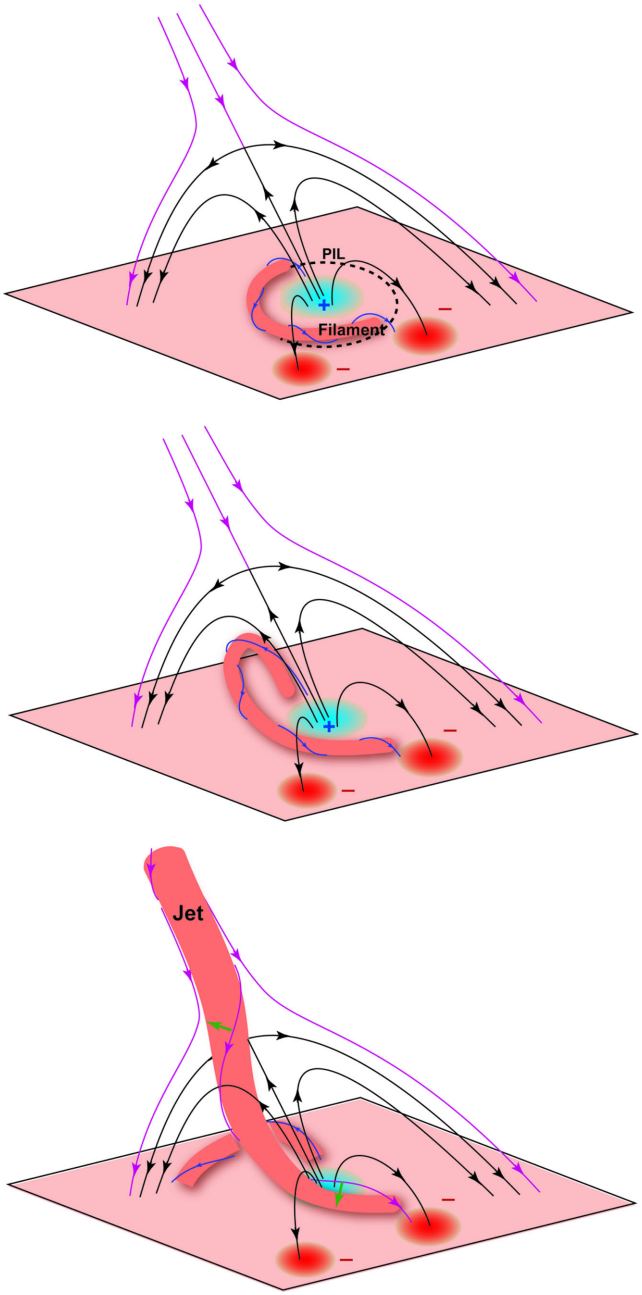

Figure 6. Magnetic configuration of the jet source region derived from *SDO* and *STEREO A* EUV images and photospheric magnetic fields distribution (upper panel). Probable scenario of the jet event (middle and lower panels).

3 DYNAMICS AND FINE STRUCTURE OF JETS

Figs 4 and 5 represent the temporal sequences of selected images showing the overall dynamics of eruption and successive jet formation in the *SDO*/AIA 171 and 304 Å channels (see also movie_171 and movie_304). The event starts from a brightening at the southern end of the filament at 23:20 UT followed by the rising of a bright loop over the middle part of the filament. The loop does not rise over the fan surface but seemingly it initiates the first blobs moving along the spine with rotation around it. Dark filament material in *SDO*/AIA 171 Å images moves to the north and rises there just below the implied coronal null point. In few minutes, the filament accelerates to a speed of the order of 100 km s^{-1}, then decelerates to a speed of about 40 km s^{-1}, and reach the height of 35 Mm, slightly below the fan surface, at 23:50 UT with even lower speed. After this time, it is difficult to recognize the top of the filament because it starts to transform into the jet. Some parts of the filament plasma are heated and becomes bright (emitting) in the *SDO*/AIA 171 and 304 Å channels. This mixture of cooler and hotter plasma starts rising along the spine direction with the clockwise rotation (if viewed from top).

Three pulses of plasma acceleration along the spine can be identified during the event. We fix the position of the leading edge of the jet and measure its coordinate along the axis of the jet (Fig. 7). The errors (standard deviations) were estimated by the three repeated measurements of the same jet's leading edge or rotating bright point. The first flow was launched by the rising bright loop at about 23:30 UT mostly as rotating separate blobs bright both in the 171 and 304 Å channel. An average speed of the blob motion along the spine has been found to be about 80 km s^{-1} (Fig. 7b). No traces of downward motion have been observed after this jet. The second jet is initiated by the dark filament eruption after 23:50 UT. It contains bright as well as dark long threads rotating clockwise. The dark threads have been observed not only in 171 Å images but also in 304 Å images, which reveal the presence of cold material. After reaching a height of 180 Mm around 00:14 UT on 2013 April 11, the most of the plasma material fall down. An average speed of rising motion is about 100 km s^{-1}, while a speed of falling down plasma is at 70 km s^{-1} (Fig. 7c). The third jet started after a new most spacious brightening near the southern end of the filament at 00:35 UT. This jet is seen most elongated and show the greatest rising averaged speed of 130 km s^{-1} (Fig. 7d).

STEREO/EUVI observations show activation of the filament within a filament channel (Fig. 8). Bright features appear in the southern section of the filament and propagate along the filament channel to the north. Saddle-like structure (Fig. 8a) projected to the north of the active region marks the position of the null point. The direction of the spine should coincide with the direction of the ambient coronal magnetic field revealed by faint coronal loops (north–north-east in this projection). The first and second jets propagate along the spine with the saddle-like structure at the base. The jets arise when bright features spreading along the filament reach the vicinity of the saddle. Bright blobs and thin dark threads can be easily recognized in *STEREO*/EUVI 195 Å images (Figs 8c–e). The main body of the third jet is rather far from the saddle structure. In this case, the connection of the jet with the southern endpoint of the filament is most obvious (Fig. 8f), although it can also be recognized in the two other jets.

The flux rope associated with the filament has the right-handed screw (positive helicity) in accordance with the sinistral chirality of the filament (Pevtsov et al. 2003; Joshi et al. 2014). Bright filament threads during its activation (Figs 8d and e) deviate clockwise from the filament axis. If they represent top sections of the helical flux tubes, as expected for the activated filament, the screw is really right-handed. Figs 9, 10 and movies show clearly the right-handed screw in the fine structure of the jet column. This indicates an unwinding of the pre-existed flux rope associated with the filament. Such unwinding is expected for an erupting flux-rope loop, since its length is increasing, while the number of helical turns remains the same.

Rotational motion of plasma blobs could also be observed in a twisted static magnetic field due to field aligned motion of the blobs. We believe that in our case we observe the rotation of the whole magnetic structure because long thin threads displace as a whole from right to left on the frontal side of the jet and from left to right on

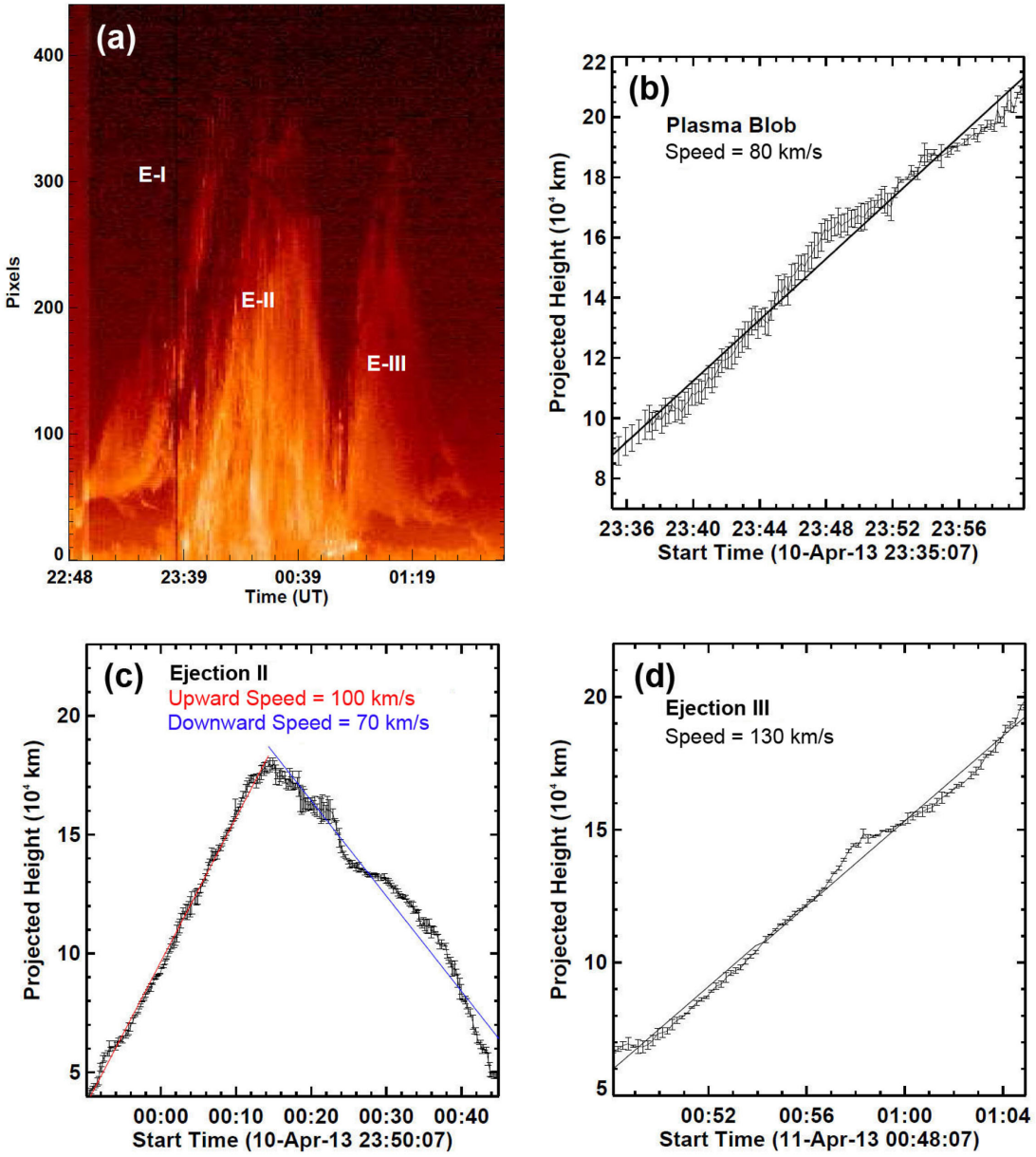

Figure 7. Time-slice diagram from cuts along the spine showing three ejections in the *SDO*/AIA 304 Å channel (a), kinematics of the three jets (b)–(c).

the far side of the jet as shown in Figs 9 and 10. Then, we measured the linear speed of rotation within jets using the displacement of tiny bright features (Fig. 11) and compared it with the averaged axial speed of plasma flows. The linear speed of rotation within the first jet was about 100 km s^{-1}, higher than speed along the spine (85 km s^{-1}). The same relationship was typical also for the second jet: 180 and 100 km s^{-1} and the third jet: 200 and 130 km s^{-1}. Taking into account the width of the jet column of about 30 Mm, the angular speed of three jets is 1.1×10^{-3}, 1.9×10^{-3} and 2.1×10^{-3} rad s^{-1}, respectively. Since the linear speed of rotation significantly exceeds the jet propagation speed, while the threads make acute angles with the jet axis, magnetic field lines move (rotate) more rapidly than plasma moves along them.

A narrow CME appeared in the north-west sector of the *SOHO*/LASCO C2 field of view at 00:00 UT on 11 April. Obviously that with an initial speed of ≈100 km s^{-1} this slow CME started long before the jet ejection. However, its position angle was very close to the position angle of the jets, thus CME's material masked a possible continuation of the jets into the upper corona.

4 DISCUSSION

In the jet event on 2013 April 10–11, we observe the rising motion of the top of the filament (presumably showing the flux-rope axis) only up to the fan surface. Then plasma moves along the general direction of the surrounding coronal magnetic field forming the jet. We can assume that the flux-rope magnetic field reconnects with the open coronal field somewhere near the coronal null point (Fig. 6). The twisted flux rope was cut in the middle part or closer to the northern end, and two halves find new connections. The southern end of the flux rope is still anchored in negative polarity to the south from the positive patch, while the other ends of these flux tubes

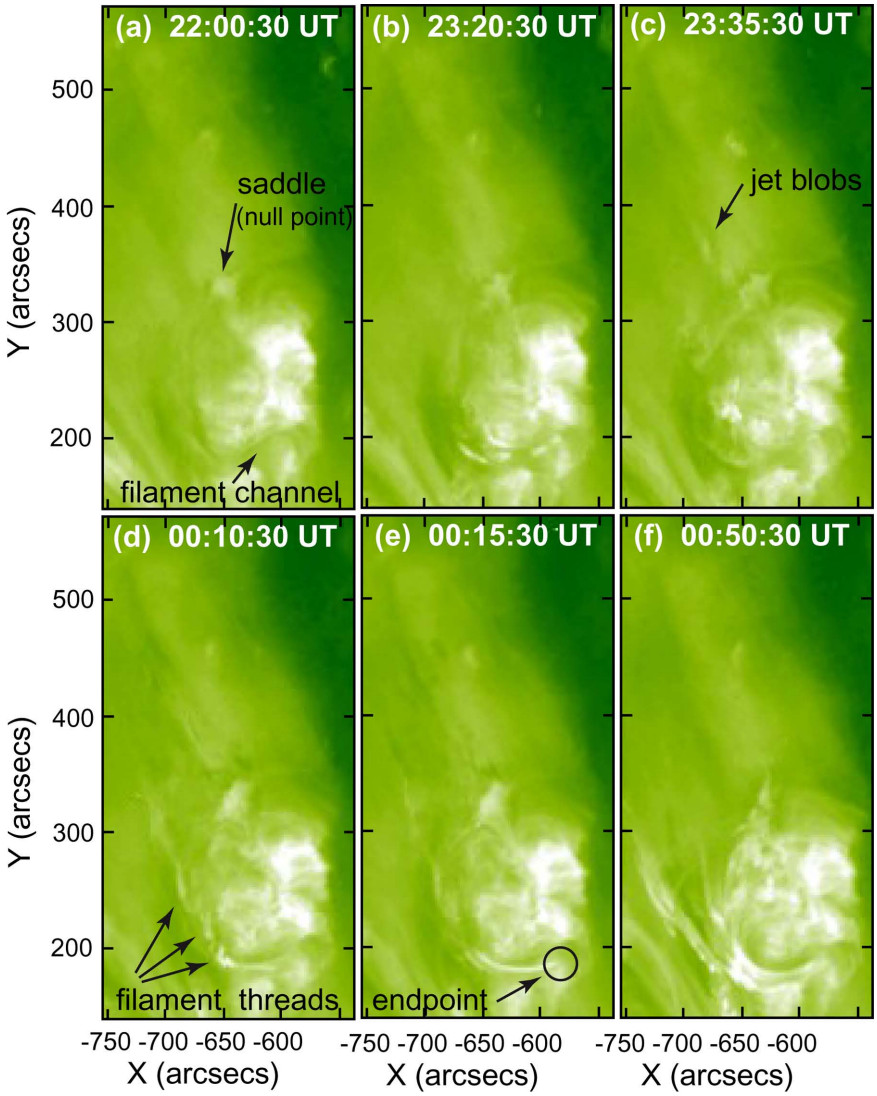

Figure 8. Selected *STEREO*/EUVI 195 Å images showing the filament eruption and jet formation.

are open to the outer corona. The southern part of the flux rope is retained at an approximately initial height by the stronger field related to the photospheric negative polarity concentrations. The northern half of the flux rope should find connection with negative polarity somewhere below the fan surface.

We have no information about evolution of photospheric magnetic fields at the base of jets just before and during their formation because the region was on the limb for magnetographic observations. Thus, we cannot relate the jet formation with emergence of new magnetic flux, as it is assumed in the majority of jet models (as well as cannot deny such relation). On the other hand, we have evidence of the presence of a flux rope in the active region before the jet event and evidence of flux-rope instability. The flux rope is disclosed by the filament. There is little doubt that filaments are enclosed within flux ropes. We can estimate the stability of flux-rope equilibrium in the coronal magnetic field knowing its height above the photosphere and calculating the so-called decay index n (Bateman 1978; Filippov & Den 2000, 2001; Kliem & Török 2006; Démoulin & Aulanier 2010; Zuccarello et al. 2014). The stable equilibrium is possible only if the background field decreases with height not too fast, or the decay index of the ambient magnetic field does not exceed a critical value n_c. Démoulin & Aulanier (2010) have shown that the critical decay index n_c has values in the range 1.1–1.3, if a flux rope expands during an upward perturbation, and in the range 1.2–1.5, if a flux rope does not expand. Horizontal equilibrium of a coronal electric current (a flux rope) is possible only at a PIL in the corona.

Fig. 12(a) represents a fragment of the magnetogram taken by the *SDO*/HMI on 2013 April 7 at 05:00 UT, which was used as a boundary condition for the potential magnetic field calculations. We solve the Neuman external boundary-value problem numerically using the Green function method (Filippov & Den 2000, 2001; Filippov 2013). Since we need the magnetic field distribution in the corona at heights of prominences, which is much less than a solar radius, we use only a restricted area of a photospheric magnetogram as the boundary of the Cartesian domain and neglect its sphericity considering as a part of a flat surface. We cut out a rectangular area around active region NOAA 1715 from the full disc magnetogram including also neighbour active region NOAA 1713 as a strong source of the magnetic field in the corona near the filament. The size of the box as seen in Fig. 12 is 600 arcsec × 577 arcsec. Since the pixel size in HMI magnetograms is about 0.5 arcsec, the size of

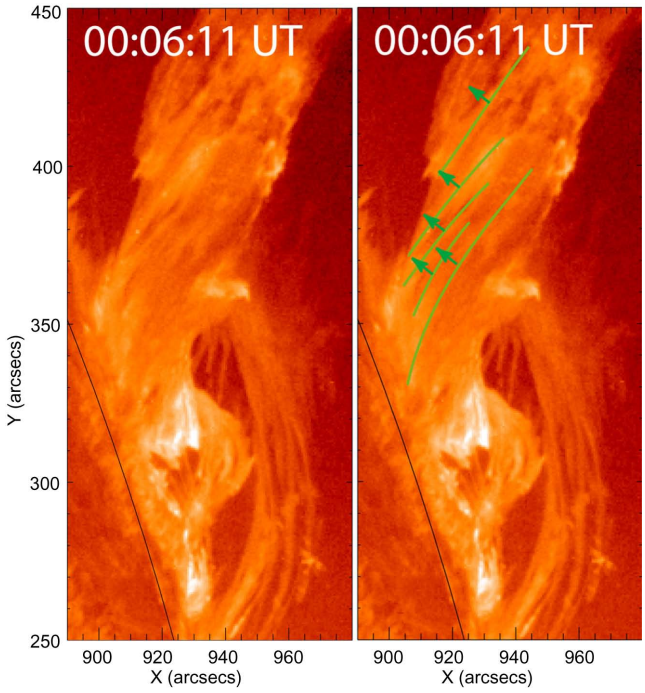

Figure 9. *SDO*/AIA 304 Å image of the jet at 00:06:11 UT. The most conspicuous threads on the frontal side of the jet are shown by green lines in the right-hand panel. Their displacements clearly seen in movie are in directions pointed by short green arrows.

the data array is 1200 × 1154. Summation over all these points in every point of the map would need rather great computational time. However, we found that for the magnetic field parameters at heights above 6 Mm the results were not changed noticeably after several binning, up to the pixel size of 8 arcsec.

Then we calculate the distribution of the decay index $n = -\mathrm{d}\ln B/\mathrm{d}\ln h$ in horizontal surfaces $h = \mathrm{const}$ at different heights h. In Figs 12(b)–(f), the thin lines show isocontours of $n = 0.5$, 1, 1.5, while the thick red lines indicate the positions of PILs at respective heights. Areas where $n > 1$ are shadowed. Blue line in Fig. 12(c) shows the section of the PIL occupied by the filament as it is seen in Hα line (Fig 3). Within a height interval from 10 to 20 Mm, there is a small volume of high values of the decay index ($n > 1.5$) near the northern end of the filament. Therefore, vertical equilibrium is not stable for the filament with the height of 13 Mm (Fig. 4 a). It should start to erupt. However, the stable equilibrium is possible again at higher heights ($\sim$ 20 Mm). We can expect a confined eruption of the filament (the flux rope) beginning in its northern section, as it is observed. The southern section of the flux rope is more stable because the decay index is small there ($n < 1$).

During such slow eruption, the flux rope stays in quasi-equilibrium. For horizontal equilibrium, it should be located near the magnetic neutral surface or at a PIL at any height. The neutral surface in NOAA 1715 has a dome-like shape as the fan surface with a smaller horizontal size than the fan surface and has the same height. The neutral surface is situated below the fan surface. They touch each other at the top, in the null point. Our potential-field calculations show the neutral surface summit at a height of 40 Mm (Fig. 12f), while the height of the fan surface top obtained from *SDO*/AIA 304 Å images is also about 40 Mm. Hence, the upper part of the slowly erupting flux rope comes to the vicinity of the null point, where there are favorable conditions for magnetic field line reconnection. Three consecutive jet ejections possibly correspond to three consecutive reconnections of separate flux tubes constituting the flux rope with open field lines above the fan surface.

We do not observe any traces of energy release near the null point during the jet formation. Bright features appear in both *STEREO* and *SDO* images within the filament body starting from the vicinity of the southern endpoint. The only observational manifestation of reconnection is a change in the field lines topology. It seems that magnetic untwisting (Shibata & Uchida 1986; Pariat et al. 2009, 2010) is the driving mechanism of plasma acceleration along the spine. One of the reasons is that the linear speed of rotation of jet features is higher than the axial speed of the jet. The sign of

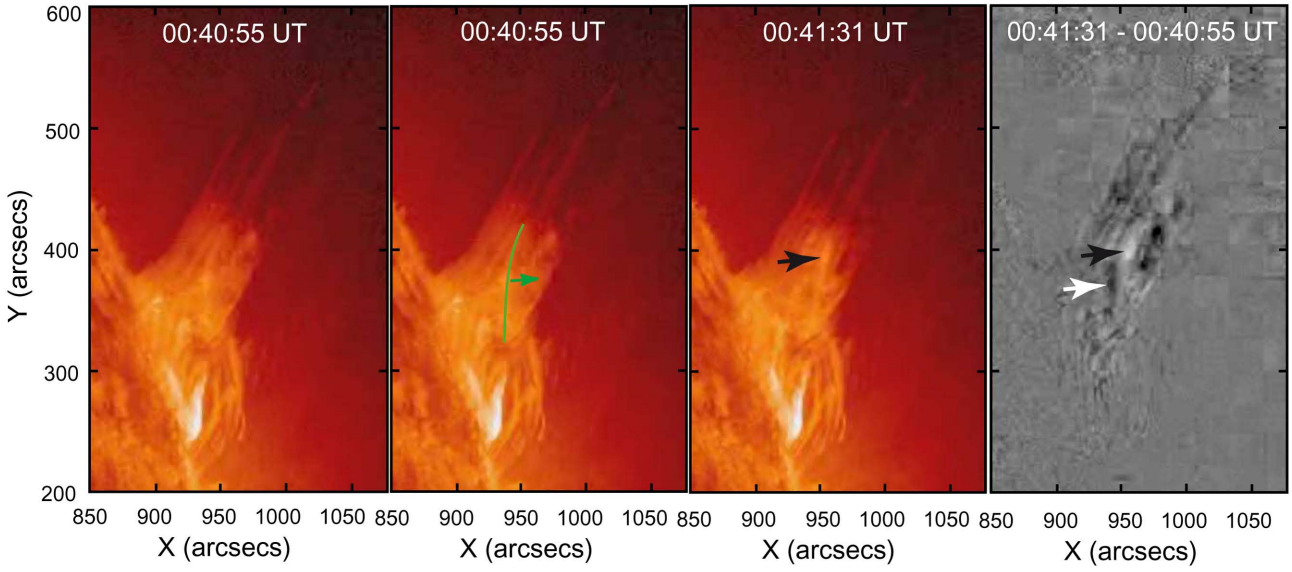

Figure 10. *SDO*/AIA 304 Å images of the jet at 00:40:55 UT and 00:41:31 UT. The bright thread marked by green line in the 00:40:55 UT snapshot and pointed by the black arrow in the 00:41:31 UT snapshot is located on the far side of the jet and moves from left to right as shown by the short green arrow. Black/white features pointed to by white/black arrows in the difference image in the right-hand panel correspond to the previous and subsequent positions of the thread.

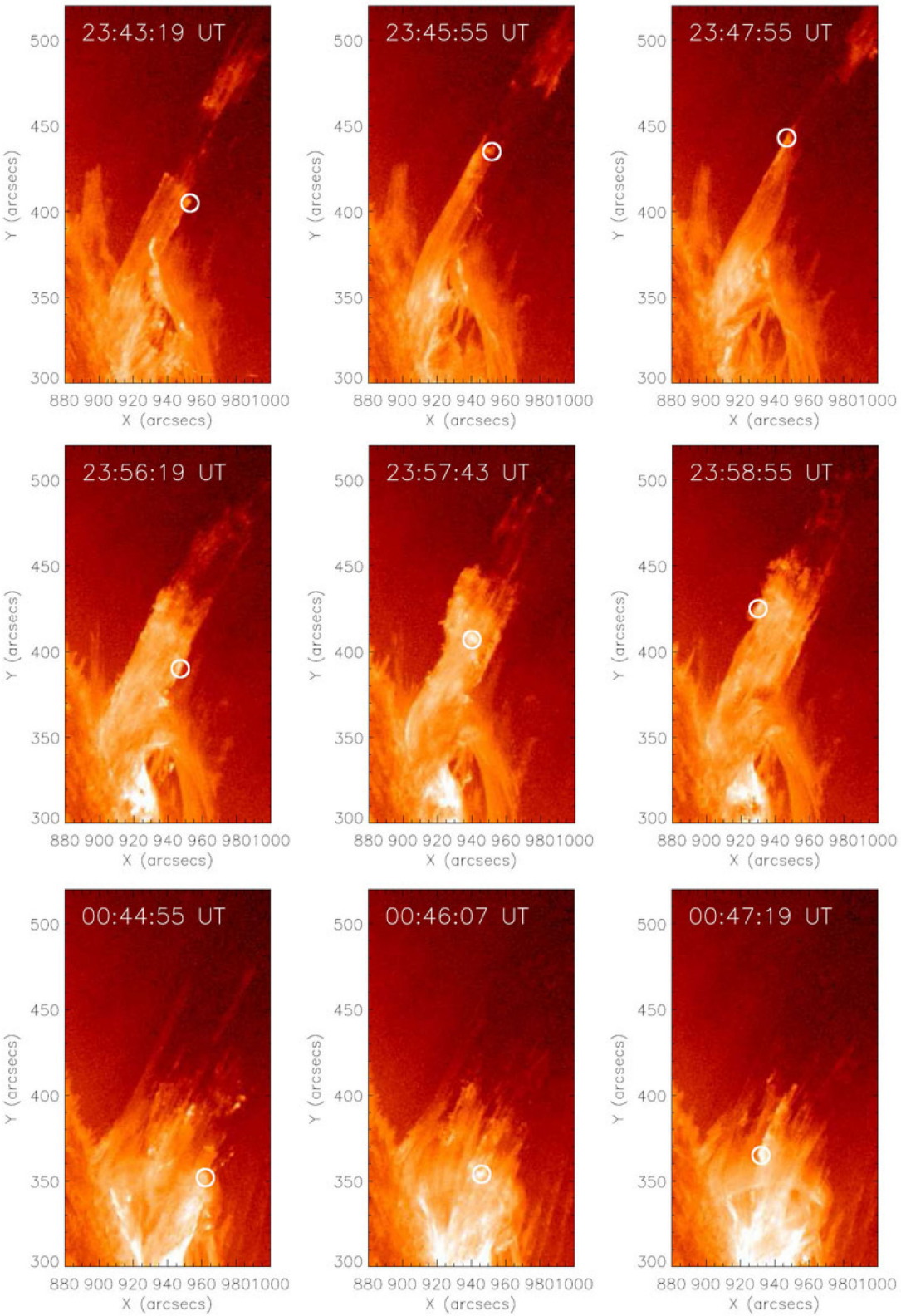

Figure 11. *SDO*/AIA 304 Å images showing the displacement of tiny bright features (within white circles) moving around the plasma column during the first (upper panel), second (middle panel) and third (bottom panel) jet-like ejection. These images were used to estimate the linear speed of rotation within jets.

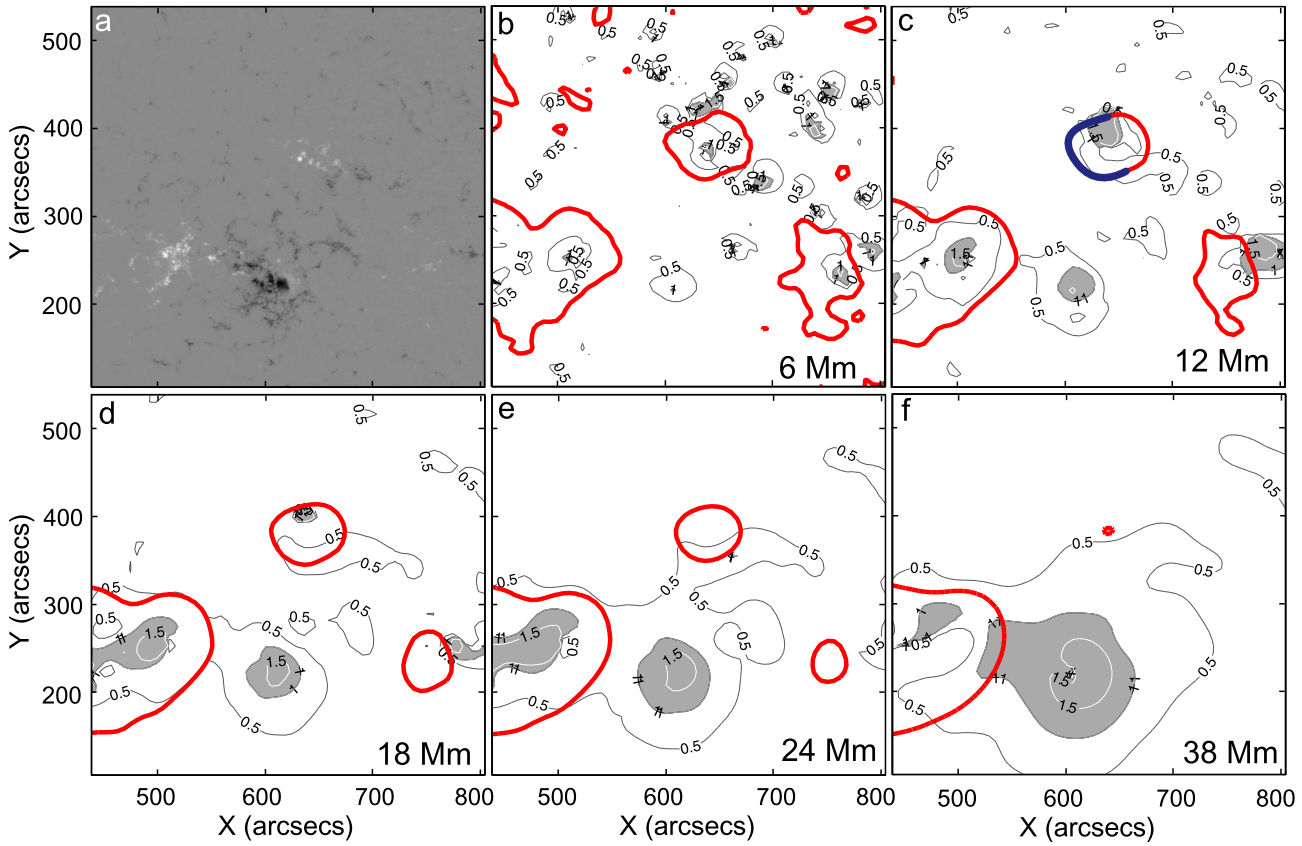

Figure 12. (a) HMI magnetogram of active regions NOAA 1713 and NOAA 1715 taken on 2013 April 07 at 05:00 UT. (Courtesy of NASA/*SDO* and the HMI science team.) (b)–(f) Distributions of the decay index and PILs (thick red lines) at different heights. Shadowed areas show the regions where $n > 1$. The section of the PIL occupied by the filament is marked with blue in (c) panel.

helicity observed in the jets corresponds to the sign of helicity of the filament, which is derived from its chirality. In this event, we have a clear example of helicity transport from a closed flux to an open flux.

Interaction of different magnetic fluxes is the necessary condition of reconnection. Usually, emergence of new flux is considered as a driver of reconnection and jet formation, although in some jet events there is no evidence of photospheric magnetic field changes during ejections (Chandrashekhar et al. 2014), or flux decrease is observed (Chifor et al. 2008). Only small changes in flux distribution showing both flux increase and decrease or slow motion of flux concentrations were found in association with jets (Liu et al. 2011; Schmieder et al. 2013). On the other hand, rapid changes in the flux distribution in the corona can be caused by instabilities of pre-existing coronal flux ropes. The presence of flux ropes in jet source regions and their eruption during jet formation is supposed in many blowout jet events (Filippov, Golub & Koutchmy 2009; Moore et al. 2010; Liu et al. 2011; Shen et al. 2011; Schmieder et al. 2013) and used as a jet driver in many models (Archontis & Hood 2013; Lee, Archontis & Hood 2015). However, observations of the pre-existing flux ropes (as filaments) are few (Shen et al. 2012; Filippov, Koutchmy & Tavabi 2013). In the jet event on 2013 April 10–11, we can identify the sinistral filament, which was observed several days before the event. The confined eruption of the filament within Eiffel tower or inverted-Y magnetic configuration led to formation of the twisted jet after reconnection at the null point between the flux rope and the external open field. The sign of helicity in the jet is the same as the sign of helicity in the filament. Untwisting motion of reconnected field lines accelerates plasma along the jet axis. The event clearly shows the twist injection from the closed pre-eruptive magnetic field of the filament to the open magnetic field of the jet.

ACKNOWLEDGEMENTS

The authors acknowledge the Kanzelhoehe Solar Observatory, *STEREO*, *SOHO* and *SDO* teams for the high-quality data supplied. This work was supported in part by the Russian Foundation for Basic Research (grant 14-02-92690) and in part by the Department of Science and Technology, Ministry of Science and Technology of India (grant INT/RFBR/P-165). BPF also acknowledges visit to Department of Physics, IIT (BHU) in 2014 November where the parts of this work is carried out.

REFERENCES

Altschuler M. D., Newkirk G., 1969, Sol. Phys., 9, 131
Archontis V., Hood A. W., 2013, ApJ, 769, L21
Bateman G., 1978, MHD Instabilities. MIT Press, Cambridge, MA
Brueckner G. E. et al., 1995, Sol. Phys., 162, 357
Canfield R. C., Reardon K. P., Leka K. D., Shibata K., Yokoyama T., Shimojo M., 1996, ApJ, 464, 1016
Chandrashekhar K., Morton R. J., Banerjee D., Gupta G. R., 2014, A&A, 562, A98
Chen H.-D., Zhang J., Ma S.-L., 2012, Res. Astron. Astrophys., 12, 573
Chifor C. et al., 2008, A&A, 491, 279
Cook J. W., Brueckner G. E., Bartoe J.-D. F., Socker D. G., 1984, Adv. Space Res., 4, 59

Démoulin P., Aulanier G., 2010, ApJ, 718, 1388
Filippov B., 2013, ApJ, 773, 10
Filippov B. P., Den O. G., 2000, Astron. Lett., 26, 322
Filippov B. P., Den O. G., 2001, J. Geophys. Res., 106, 25177
Filippov B., Golub L., Koutchmy S., 2009, Sol. Phys., 254, 259
Filippov B., Koutchmy S., Tavabi E., 2013, Sol. Phys., 286, 143
Heyvaerts J., Priest E. R., Rust D. M., 1977, ApJ, 216, 123
Howard R. A. et al., 2008, Space Sci. Rev., 136, 67
Isobe H., Tripathi D., Archontis V., 2007, ApJ, 657, L53
Joshi N. C., Srivastava A. K., Filippov B., Kayshap P., Uddin W., Chandra R., Choudhary D. P., Dwivedi B. N., 2014, ApJ, 787, 11
Kliem B., Török T., 2006, Phys. Rev. Lett., 96, 255002
Kurokawa H., Hanaoka Y., Shibata K., Uchida Y., 1987, Sol. Phys., 108, 251
Lee E. J., Archontis V., Hood A. W., 2015, ApJ, 798, L10
Lemen J. R. et al., 2012, Sol. Phys., 275, 17
Liu W., Berger T. E., Title A. M., Tarbell T. D., 2009, ApJ, 707, L37
Liu C., Deng N., Liu R., Ugarte-Urra I., Wang S., Wang H., 2011, ApJ, 735, L18
Moore R. L., Cirtain J. W., Sterling A. C., Falconer D. A., 2010, ApJ, 720, 757
Moreno-Insertis F., Galsgaard K., 2013, ApJ, 771, 20
Pariat E., Antiochos S. K., DeVore C. R., 2009, ApJ, 691, 61
Pariat E., Antiochos S. K., DeVore C. R., 2010, 714, 1762
Pariat E., DeVore C. R., Dalmasse K., Antiochos S. K., Karpen J. T., 2015, A&A, 573, A130
Patsourakos S., Pariat E., Vourlidas A., Antiochos S. K., Wuelser J. P., 2008, ApJ, 680, L73
Pevtsov A. A., Balasubramaniam K. S., Rogers J. W., 2003, ApJ, 595, 500
Pike C. D., Mason H. E., 1998, Sol. Phys. 182, 133
Schatten K. H., Wilcox J. M., Ness N. F., 1969, Sol. Phys., 6, 442
Schmieder B. et al., 2013, A&A, 559, A1
Schou J. et al., 2012, Sol. Phys., 275, 229
Schrijver C. J., DeRosa M. L., 2003, Sol. Phys., 212, 165
Shen Y., Liu Y., Su J., Ibrahim A., 2011, ApJ, 735, L43
Shen Y., Liu Y., Su J., Deng Y., 2012, ApJ, 745, 164
Shibata K., 1998, in Guyenne T.-D., ed., ESA SP-421: Solar Jets and Coronal Plumes. ESA, Noordwijk, p. 137
Shibata K., Uchida Y., 1986, Sol. Phys., 103, 299
Shibata K. et al., 1992, PASJ, 44, L173
Shibata K., Nozawa S., Matsumoto R., 1992, PASJ, 44, 265
Shimojo M., Hashimoto S., Shibata K., Hirayama T., Hudson H. S., Acton L., 1996, PASJ, 48, 123
Steiolfson R. S., Schmahl E. J., Wu S. T., 1979, Sol. Phys., 63, 187
Sterling A. C., Harra L. K., Moore R. L., 2010, ApJ, 722, 1644
Suematsu Y., Shibata K., Nishikawa T., Kitai R., 1982, Sol. Phys., 75, 99
Wang H., Liu C., 2012, ApJ, 760, 101
Wuelser J.-P. et al., 2004, in Fineschi S., Gummin M. A., eds, Proc. SPIE Conf. Ser. Vol. 5171, Telescopes and Instrumentation for Solar Astrophysics. SPIE, Bellingham, p. 111
Xu A.-A., Yin S.-Y., Ding J.-P., 1984, Acta Astron. Sin., 25, 119
Yokoyama T., Shibata K., 1996, PASJ, 48, 353
Zuccarello F. P., Seaton D. B., Mierla M., Poedts S., Rachmeler L. A., Romano P., Zuccarello F., 2014, ApJ., 785, 88

SUPPORTING INFORMATION

Additional Supporting Information may be found in the online version of this article:

movie_304.mpeg
movie_171.mpeg (http://mnras.oxfordjournals.org/lookup/suppl/doi:10.1093/mnras/stv1039/-/DC1).

Please note: Oxford University Press are not responsible for the content or functionality of any supporting materials supplied by the authors. Any queries (other than missing material) should be directed to the corresponding author for the article.

This paper has been typeset from a TEX/LATEX file prepared by the author.